Synthesis and Characterization of *N*- and *O*-Alkylated Poly[aniline-*co*-*N*-(2-hydroxyethyl) aniline]

Leyla Shadi,[1] Homa Gheybi,[1] Ali Akbar Entezami,[1] Kazem D. Safa[2]

[1]*Laboratory of Polymer, Faculty of Chemistry, University of Tabriz, Tabriz, Iran*
[2]*Laboratory of Organo Silicone, Faculty of Chemistry, University of Tabriz, Tabriz, Iran*

Received 21 November 2010; accepted 8 July 2011
DOI 10.1002/app.35218
Published online 26 October 2011 in Wiley Online Library (wileyonlinelibrary.com).

ABSTRACT: Poly[aniline-*co*-*N*-(2-hydroxyethyl) aniline] was synthesized in an aqueous hydrochloric acid medium with a determined feed ratio by chemical oxidative polymerization. This polymer was used as a functional conducting polymer intermediate because of its side-group reactivity. To synthesize the alkyl-substituted copolymer, the initial copolymer was reacted with NaH to obtain the *N*- and *O*-anionic copolymer after the reaction with octadecyl bromide to prepare the octadecyl-substituted polymer. The microstructure of the obtained polymers was characterized by Fourier transform infrared spectroscopy, ^{1}H-NMR, and X-ray diffraction. The thermal behavior of the polymers was investigated by thermogravimetric analysis and differential scanning calorimetry. The morphology of obtained copolymers was studied by scanning electron microscopy. The cyclic voltammetry investigation showed the electroactivity of poly [aniline-*co*-*N*-(2-hydroxyethyl) aniline] and *N* and *O*-alkylated poly[aniline-*co*-*N*-(2-hydroxyethyl) aniline]. The conductivities of the polymers were 5×10^{-5} S/cm for poly[aniline-*co*-*N*-(2-hydroxyethyl) aniline] and 5×10^{-7} S/cm for the octadecyl-substituted copolymer. The conductivity measurements were performed with a four-point probe method. The solubility of the initial copolymer in common organic solvents such as *N*-methyl-2-pyrrolidone and dimethylformamide was greater than polyaniline. The alkylated copolymer was mainly soluble in nonpolar solvents such as *n*-hexane and cyclohexane. © 2011 Wiley Periodicals, Inc. J Appl Polym Sci 124: 2118–2126, 2012

Key words: conducting polymers; conjugated polymers; functionalization of polymers; graft copolymers; polymer synthesis and characterization

INTRODUCTION

During the past 3 decades, a wide variety of electrically conducting polymers have been studied because of their exclusive physical properties. Among the conducting polymers, including polyaniline, polypyrrole, polythiophene, and polyacetylene, polyaniline has been studied extensively for its environmental stability in the conducting form, easiness in synthesis, low-cost synthesis, unique redox properties, and reasonable conductivity.[1] These properties are favorable for its applications in gas sensing,[2–4] solar cells,[5,6] electromagnetic interference shielding,[7,8] antistatic coating,[9] and organic light-emitting diodes.[10–12] However, for a long time, it has been revealed to be difficult to process, having no solubility and melting point, likely because of its intrinsic stiffness. Numerous methods have been developed to overcome these shortcomings. These include

- The postprocessing technique.[13]
- Emulsion polymerization.[14–16]
- Preparation of the composites or blends.[17–19]
- Copolymerization.[20,21]
- The incorporation of side groups into the main chain.[22–25]
- The grafting of electron-donating groups, such as alkyl groups.[26–28]

Among these methods, important chemical modifications have been the copolymerization and addition of saturated hydrocarbon alkyl side chains to the polymeric backbone. These approaches have been successfully applied to solubilize the intractable polyaniline with the copolymerization of aniline with other monomers and the incorporation of alkyl groups with various sizes. Zheng et al.[26] reported the incorporation of alkyl side chains into the polyaniline backbone. They showed that the incorporation of alkyl substituents in various sizes could control the chemical structure, innovate in its tractability for processing applications, and modify the physical properties of this conjugated polymer. In addition, the improvement of solubility in common organic solvents for products with more than eight carbons on the side chain was proven. Cataldo and Maltese[29] made a complete investigation of the thermal stability of PANI and its alkyl and *N*-alkyl derivatives in the undoped state, known as *emeraldine base*, and in the doped state, where camphorsulfonic acid (CSA) was used as a dopant for its applications in a gas-sensing device. Recently, the synthesis and characterization of

Correspondence to: A. A. Entezami (aaentezami@yahoo.com or aentezami@tabrizu.ac.ir).

copolymers of aniline with *o*- and *m*-toluidine was investigated by Savitha and Sathyanarayana.[30] They found that copolymers of aniline with *o*-toluidine showed a greater resemblance to the poly(*o*-toluidine) homopolymer; this may have been due to the higher amounts of *o*-toluidine in the copolymers. This led to an increase in the solubility but a lowering of the conductivity. The development of a new chemical method that allows more general access to pure polyaniline derivatives was reported by Falcou et al.[27] They presented the synthesis of poly(*ortho*-alkyl anilines) and poly(*N*-alkyl anilines) bearing various alkyl chains in a mixture of hexane, water, and tetrahydrofuran. The properties of these materials, including solubility and thermal behavior, were compared and correlated with the substituent nature of the polymers. The effects of the side-chain length on the physical properties were investigated by spectroscopic and steric exclusion chromatography measurements.

In this work, we demonstrated the synthesis and properties of soluble poly[aniline-*co*-*N*-(2-hydroxyethyl) aniline]. This copolymer could be used as a functional conducting polymer intermediate because of the reactive hydroxyethyl side groups. Also, we investigated the modification of the resulting copolymer by the electrophilic substitution of the *N*-hydrogen and *O*-hydrogen atoms of the copolymer. Precisely, we focused on the solubility, thermal behavior, and electrochemical properties.

EXPERIMENTAL

Materials

Hydrochloric acid was received from Merck (Germany). Aniline from Merck was distilled *in vacuo* and stored under a nitrogen atmosphere in the dark before polymerization. Fresh ammonium persulfate and NaH were purchased from Merck. *N*-(2-Hydroxyethyl) aniline and octadecyl bromide (Aldrich, USA) were used without further purification. Dimethyl sulfoxide (DMSO) was completely dried and then distilled under reduced pressure.

Synthesis of poly[aniline-*co*-*N*-(2-hydroxyethyl) aniline]

Poly[aniline-*co*-*N*-(2-hydroxyethyl) aniline] was prepared by chemical polymerization with a mixture of aniline and *N*-2-hydroxyethyl aniline in an aqueous solution of 1*M* hydrochloric acid with ammonium persulfate as an oxidant. The molar fraction of aniline to *N*-2-hydroxyethyl aniline was 1 : 1. In this case, the molar ratio of oxidant to total monomers was 1. A typical polymerization procedure is outlined as follows: aniline (4.55 mL) and *N*-2-hydroxyethyl aniline (6.26 mL) were dissolved in 100 mL of 1*M* HCl aqueous solution. Ammonium persulfate (22.8 g), dissolved in 100 mL of a 1*M* HCl aqueous solution, was then added dropwise to the solution with constant stirring. After 15 h, the green-colored copolymer was filtered out and washed with methanol and distilled water until the filtered solution became colorless. The green powder thus obtained was dried *in vacuo* at 50°C for 48 h. The copolymer was treated with an aqueous NH_3 solution to obtain the neutralized form. The HCl-doped copolymer (0.5 g) was suspended in 100 mL of 3% NH_3 with stirring for 2 h. The mixture was then filtered, washed with distilled water and methanol, and then dried *in vacuo* for 48 h (yield = 60%).

Synthesis of *N*- and *O*-alkylated copolymer

For preparation of the alkylated copolymer with octadecyl bromide, the reaction flask was dried and kept under an inert atmosphere throughout the reactions by a constant flow of argon. NaH (0.129 g, 0.0054 mol) was dissolved in 40 mL of dried DMSO. The solution was stirred under an argon atmosphere at 60°C until the NaH was completely dissolved. The copolymer (0.5 g) was added and constantly stirred for 4 h. Then, the solution was cooled to 40°C and 2.22 g of octadecyl bromide was added, and the reaction was continued for a further 18 h. The reaction mixture was poured into methanol to precipitate the substituted copolymer. The precipitate was filtered, washed with methanol, and then refluxed in acetone to remove the residual amount of unreacted alkyl bromide. Finally, the polymer was dried in a vacuum oven at 50°C (yield = 55%).

Characterization

The copolymer composition was determined from the 1H-NMR spectra (Bruker 400-MHz spectrometer,Germany) with tetramethylsilane as an internal reference. The initial copolymer was dissolved in hexadeuterated dimethyl sulfoxide (DMSO-d_6), whereas the alkylated copolymer was dissolved in $CDCl_3$ because of its poor solubility in DMSO. Fourier transform infrared (FTIR) spectra were recorded with a Shimadzu FTIR-8101 M spectrometer(Japan). The samples were prepared in the pellet form with spectroscopic-grade KBr powder. The phase transitions were investigated over the range 0–300°C in a nitrogen atmosphere with a Netzsch DSC 200 F3 differential scanning calorimeter(Germany) at a heating rate of 10°C/min. The instrument was calibrated with indium for temperature and enthalpy. The HCl-doped copolymer was compressed into disks with a diameter of 10 mm and a thickness of 100 μm with a pellet maker. The direct current electrical conductivities of the disk specimens were measured with

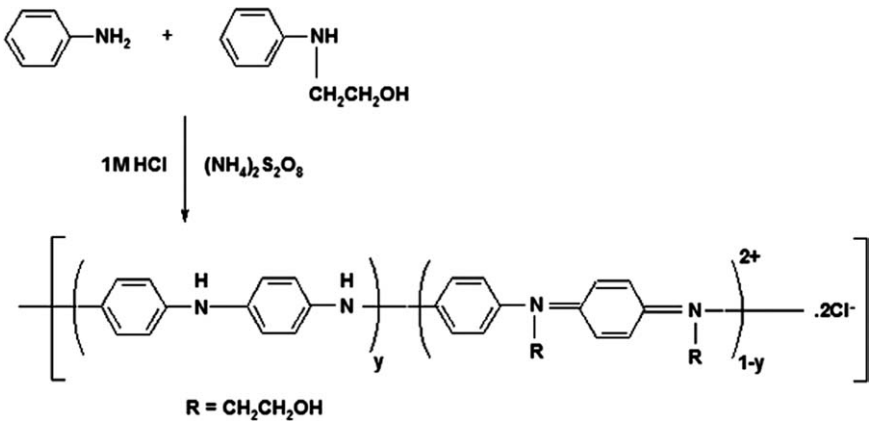

Scheme 1 Synthesis outline of aniline and the *N*-(2-hydroxyethyl) aniline copolymer.

a four-point method. The thermal stability of the copolymers was measured with a PerkinElmer thermogravimetric analysis (TGA) instrument (Pyrise Diamond thermogravimetric/differential thermal analyzer,USA) under a nitrogen atmosphere at a heating rate of 10°C/min. The poly[aniline-*co*-*N*-(2-hydroxyethyl) aniline] and alkylated copolymer samples were mounted on metal stubs and coated with gold, and their surfaces were observed and photographed by a scanning electron microscope (LEO 14557p, England). X-ray diffraction (XRD) analyses of the copolymers were performed on a Siemens X-ray diffractometer (model D5000,Germany) with Cu Kα radiation at 40 kV and 30 mA. Data were collected at a scanning rate of 0.3°/min. The electrochemical properties of the films of the polymers coated on platinum foil electrodes were studied in a one-compartment cell equipped with a platinum wire counter electrode and an Ag/AgCl (3.8 N KCl) reference electrode. Cyclic voltammograms were recorded with an AUTOLAB PGSTAT 30 electro-chemical analysis system and the GPES 4.7 software package (Eco Chemie, The Netherlands).

RESULTS AND DISCUSSION

The copolymerization of aniline and *N*-(2-hydroxyethyl) aniline in 1 : 1 monomer molar feed ratios was carried out easily by chemical oxidative polymerization with ammonium persulfate. The process for synthesis of the copolymer is shown in Scheme 1. As a result of the hydroxyethyl side groups, the copolymer had more solubility in organic solvents such as *N*-methyl-2-pyrrolidone (NMP) and dimethylformamide (DMF). Also, this polymer could be used as a functional conducting polymer with the reactivity of the side groups. Then, this functional copolymer was reacted with octadecyl bromide to produce *N*- and *O*-alkylated copolymer, as shown in Scheme 2. Interestingly, the solubility of the alkylated copolymer was completely changed, and it

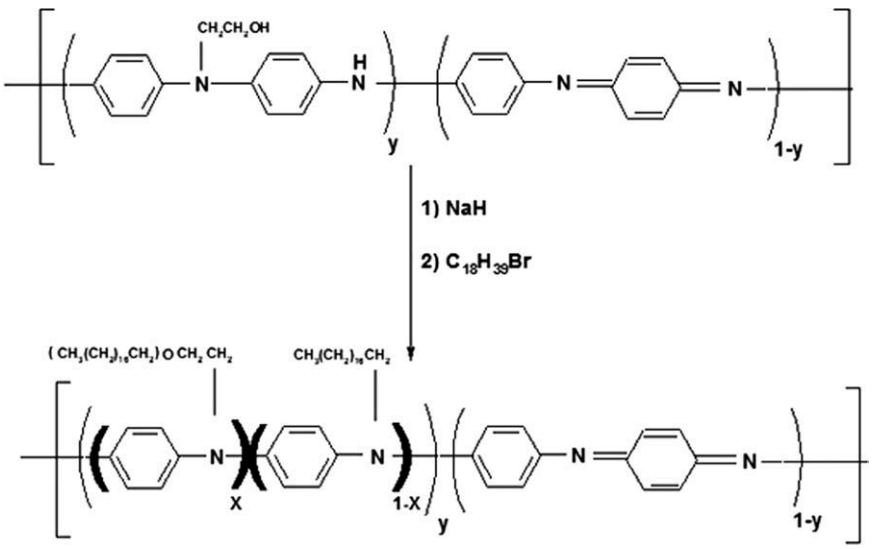

Scheme 2 Synthesis route of the alkylation of poly[aniline-*co*-*N*-(2-hydroxyethyl) aniline].

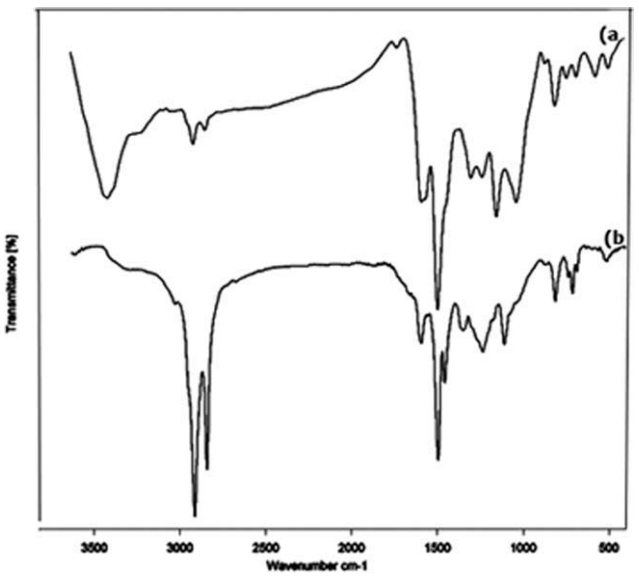

Figure 1 FTIR spectra of the synthesized copolymers: (a) poly[aniline-*co*-*N*-(2-hydroxyethyl) aniline] and (b) alkylated copolymer.

was soluble in nonpolar solvents such as *n*-hexane and cyclohexane.

FTIR and ^{1}H-NMR spectroscopy

The copolymer composition was studied by ^{1}H-NMR and FTIR spectroscopy. Representative FTIR spectra for the copolymer of aniline and *N*-(2-hydroxyethyl) aniline with molar ratios of 1 : 1 and alkylated form are shown in Figure 1. The initial copolymer exhibited numerous characteristic bands common to polyaniline. A vibrational peak at 1593 cm^{-1} was assigned to the stretching of the quinoid (Q) ring, and a peak at 1498 cm^{-1} was attributed to the stretching of the benzenoid ring. The presence of the quinoid ring was also suggested by the peak at 1156 cm^{-1}, which was characteristic of the electronic-like absorption of the N=Q=N vibration. The —C—H out-of-plane bending vibrations of the 1,4-disubstituted aromatic ring appeared at 816 cm^{-1}, which represented additional evidence for the presence of benzenoid rings. However, the main differences occurred between the 2800 and 3500 cm^{-1} regions (O—H and C—H stretching bands). Symmetric and asymmetric aliphatic C—H stretching was observed at 2856 and 2924 cm^{-1}, respectively; this originated from the hydroxyethyl substituent of the *N*-(2-hydroxyethyl) aniline unit. In addition, —O—H stretching of the hydroxyethyl substituent appeared at 3422 cm^{-1}; this indicated that this group was in the intramolecular and intermolecular hydrogen-bonded states. This indicated that the monomers of *N*-(2-hydroxyethyl) aniline and aniline were, indeed, incorporated into the copolymer. A close comparison of the spectrum of the copolymer [Fig. 1(a)] with the alkylated copolymer [Fig. 1(b)] revealed the differences between them. The bands around 2856 and 2924 cm^{-1} showed wide variations in intensity after the grafting of octadecyl groups. Furthermore, another noticeable feature in the spectrum was the disappearance of absorption bands around 3422 cm^{-1}, which corresponded to —O—H stretching and the presence of aliphatic C—N stretching at 1242 cm^{-1}. These observations confirmed the grafting of the alkyl groups onto the copolymer backbone.

Supporting evidence for the structural elucidation was revealed by ^{1}H-NMR analysis. The ^{1}H-NMR spectrum of poly[aniline-*co*-*N*-(2-hydroxyethyl) aniline] in DMSO-d_6 is shown in Figure 2(a). Spectral features indicative of the hydroxyethyl side groups were present. The signals in the region 2.4–2.5 ppm were due to the protons of methylene in the side chain, whereas the signal at 3.3–3.5 ppm was due to

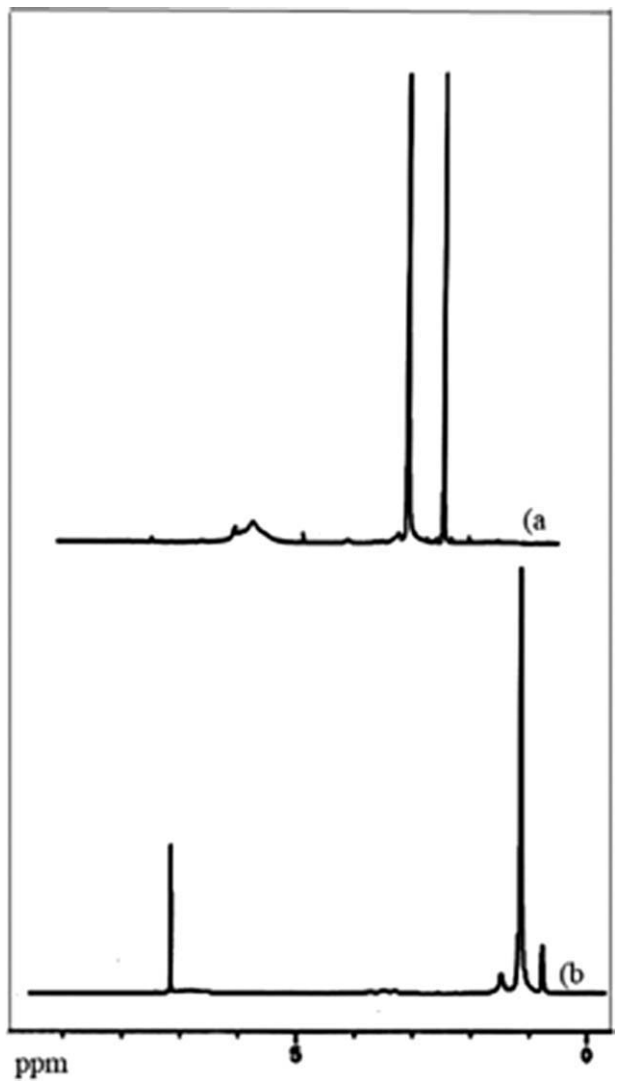

Figure 2 ^{1}H-NMR spectra of (a) poly[aniline-*co*-*N*-(2-hydroxyethyl) aniline] in DMSO-d_6 and (b) alkylated form of poly[aniline-*co*-*N*-(2-hydroxyethyl) aniline] in $CDCl_3$.

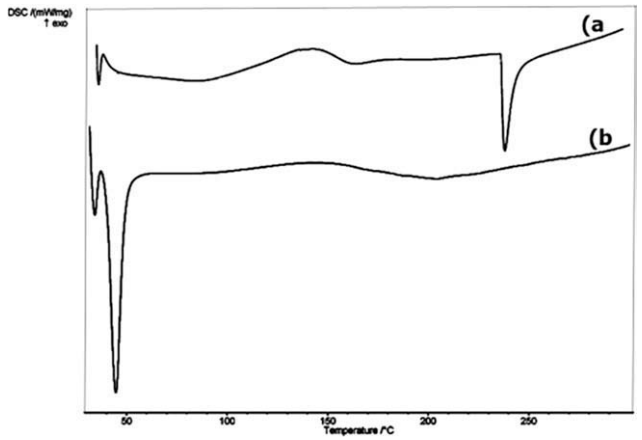

Figure 3 DSC thermograms measured from (a) poly[aniline-*co*-*N*-(2-hydroxyethyl) aniline] and (b) the alkylated form of poly[aniline-*co*-*N*-(2-hydroxyethyl) aniline].

the protons of —CH_2O— groups. The resonance at 4.7 ppm could be assigned to the hydroxyl protons, and those in the region 6.3–7.5 ppm could be assigned to the protons of the quinoid and aromatic rings. Figure 2(b) displays the ^{1}H-NMR spectrum of the alkylated copolymer in $CDCl_3$. This copolymer had poor solubility in DMSO after the grafting of alkyl groups. According to this figure, the appearance of a peak at 0.8 ppm could be attributed to the methyl protons of alkyl groups in the side chains. In addition, the resonance near 1.2 ppm was assigned to CH_2 groups of the alkyl chain. The peak in the region 3.4–3.6 ppm was related to —CH_2O— group. The decrease in the intensity of the peak —CH_2O— group in the alkylated copolymer had two reasons. First, ^{1}H-NMR spectra of the copolymers were recorded in different solvents. Poly[aniline-*co*-*N*-(2-hydroxyethyl) aniline] and the alkylated copolymer were dissolved in DMSO-d_6 and $CDCl_3$, respectively. Also, the grafting of the long alkyl group in the alkylated polymer may have decreased the intensity of the —CH_2O— group because of connection of this group to the 18 carbon. Furthermore, aromatic protons were detected at 6.9–7 ppm that overlapped with resonances of the solvent. Overall, the results indicate a successful formation of the initial copolymer and alkylated form.

Thermal analysis

Differential scanning calorimetry (DSC) analysis

The DSC trace of the poly[aniline-*co*-*N*-(2-hydroxyethyl) aniline] powder showed three endothermic peaks at 25–40, 140–180, and 230–250°C, as shown in Figure 3(a). The first peak was due to the evaporation of absorbed volatile molecules. The second peak could be attributed to the decomposition of the hydroxyethyl side groups. The third endothermic peak (230–250°C) agreed with the crosslinking reaction of the coupled quinoid rings in the polymers.[20] In the DSC curve of the alkylated copolymer, three endothermic peaks were also observed [Fig. 3(b)], one at 25–40°C, which arose from the evaporation of volatile molecules, and the second at 40–50°C, which arose from the melting of octadecyl groups. This thermogram also showed another endothermic peak at 160–250°C. This peak could be attributed to the crosslinking reaction of the coupled quinoid rings in the polymers.[20] The performance of this reaction was confirmed by weight loss results discussed later in this article.

TGA

The results of the TGA of poly[aniline-*co*-*N*-(2-hydroxyethyl) aniline] and alkylated copolymer are plotted in Figure 4(a,b), respectively. As shown, the TGA patterns of the copolymers had obvious differences. Poly[aniline-*co*-*N*-(2-hydroxyethyl) aniline] showed a three-step weight loss behavior. The first weight loss occurred at 30–90°C; this was attributed to a loss of the removal of residual solvents and small molecules. The second step was observed in the temperature range 100–300°C; this may have been due to the degradation of the hydroxyethyl side groups. The final step at higher temperatures (>350°) may have been due to the decomposition of the polymer backbone.

In the alkylated copolymer, the TGA curve changed completely and exhibited two step of degradation, one of which was a weight loss around 210–280°C, which could have been due to the alkyl side group, and another one above 300°C that may have been caused by the decomposition of the polymer backbone. Moreover, Figure 5 shows the differential thermal analysis (DTA) of the alkylated copolymer. The alkylated copolymer showed two endothermic peaks; the first one was around 30°C; this was attributed to the melting of the crystalline structure formed by the side groups because octadecane crystal had a melting point around 40–50°C.[31] Also, the other endothermic peak above 400°C could have been due to the degradation of the polymer backbone. These differences in the

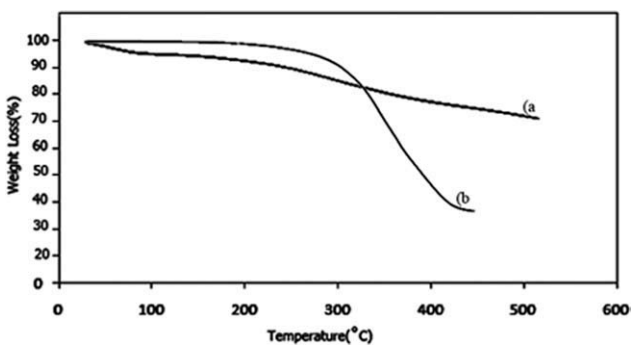

Figure 4 TGA thermograms of the copolymers: (a) poly[-aniline-*co*-*N*-(2-hydroxyethyl) aniline] and (b) the alkylated copolymer.

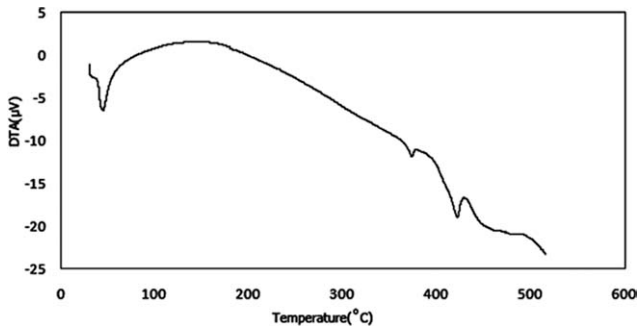

Figure 5 DTA thermogram measured from octadecylated poly[aniline-*co*-*N*-(2-hydroxyethyl) aniline].

thermal behavior of the copolymers confirmed the accomplishment of the reaction and the modification of the initial structure.

Solubility

Poly[aniline-*co*-*N*-(2-hydroxyethyl) aniline] exhibited better solubility in NMP and DMF, as shown in Table I. The improved solubility of this copolymer over polyaniline appeared to be related to the introduction of the functional groups onto the polymer backbone. In contrast to poly[aniline-*co*-*N*-(2-hydroxyethyl) aniline], the alkylated copolymer, with alkyl groups having a carbon number of 18, exhibited good solubility in common nonpolar organic solvents. The increase in solubility could be attributed to the decrease in polarity and the stiffness of the polymer chains caused by the incorporation of the flexible alkyl side chains. As shown in Table I, highly polar solvents, such as NMP and DMF, which were good solvents for the initial copolymer, were no longer good solvents for the alkylated form; this resulted from the lack of amine hydrogen in the alkylated copolymer to provide hydrogen-bonding interaction with and solvation by the solvents, which diminished their solubility in polar solvents.[32]

Scanning electron microscopy (SEM)

SEM was used to characterize the morphology of the copolymer samples. As shown in Figure 6, SEM

TABLE I
Solubility of the Copolymers in Common Organic Solvents

Sample	NMP	DMF	THF	$CHCl_3$	*n*-Hexane
Poly[aniline-*co*-*N*-(2-hydroxyethyl) aniline]	+	+	−	−	−
Octadecylated poly [aniline-*co*-*N*-(2-hydroxyethyl)aniline]	−	−	+	+	+

+, mainly soluble; −, insoluble.

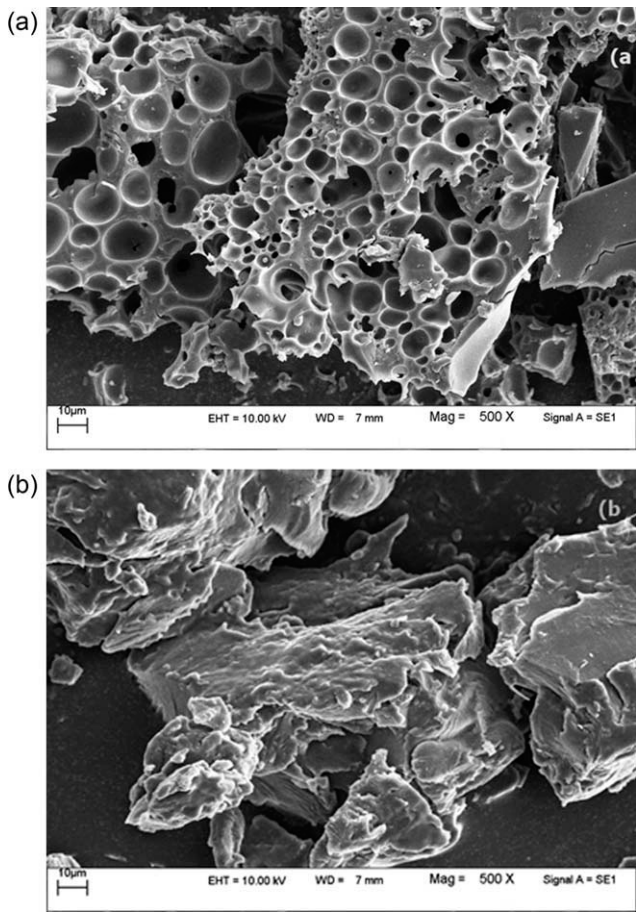

Figure 6 SEM of (a) poly[aniline-*co*-*N*-(2-hydroxyethyl) aniline] and (b) the octadecylated copolymer.

revealed some variations in the morphological structure of poly[aniline-*co*-*N*-(2-hydroxyethyl) aniline] and the octadecyl-substituted copolymer sample. The initial copolymer exhibited a porous morphology, which may have originated from the presence of hydroxyl side groups in the polymer backbone. The hydroxyl side groups had intramolecular interactions with H_2O molecules. In a high vacuum (the SEM analysis was performed in a high vacuum), the evaporation of H_2O molecules from the bulk of the copolymer may have led to a porous structure. In the alkyl-grafted sample, the microstructure of the copolymer was completely changed, whereas the porous morphology of the initial copolymer disappeared. This variation could be explained by the substitution of alkyl chains onto the nitrogen and oxygen atoms of the copolymer backbone, which converted the hydroxyl side groups to ether groups and resulted in a bulky structure in the octadecylated copolymer.

XRD

Figure 7 presents XRD patterns measured from the initial copolymer and alkylated form films. Poly[aniline-*co*-*N*-(2-hydroxyethyl) aniline] exhibited broad

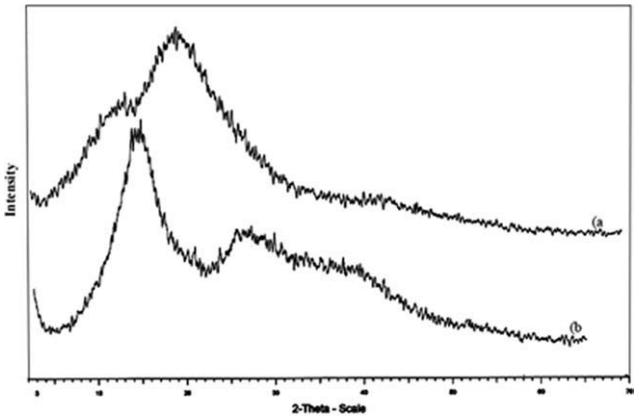

Figure 7 XRD patterns of the copolymers: (a) poly[aniline-*co*-*N*-(2-hydroxyethyl) aniline] and (b) the alkylated copolymer.

peaks in the XRD pattern at 11.2 and 20° (2θ). The peak at 11.2°, related to the small side chains as hydroxyl groups, was weaker than the other peak. After alkylation, the XRD pattern of the copolymer showed basic variations. The octadecylated copolymer showed two peaks around 15 and 27° (2θ). The presence of the peak at 27° could be explained by the formation of an ordered structure after the reaction of the initial copolymer with octadecyl bromide. The increasing order in the final structure could have originated from the octadecane crystal side groups, which affected the manner of the layers' arrangement. Also, in the DSC curve of the alkylated copolymer, the peak at 40–50°C was attributed to the octadecane crystals. The presence of this peak also proved the increase of order in the final copolymer.

Electrochemical properties

The thin films of the copolymers were prepared on platinum electrode by casting. A three electrode cell was employed by using platinum foil as working electrode (2 mm), platinum wire as counter electrode and Ag/AgCl as reference electrode. The oxidation potentials of the polymers were determined in 1M

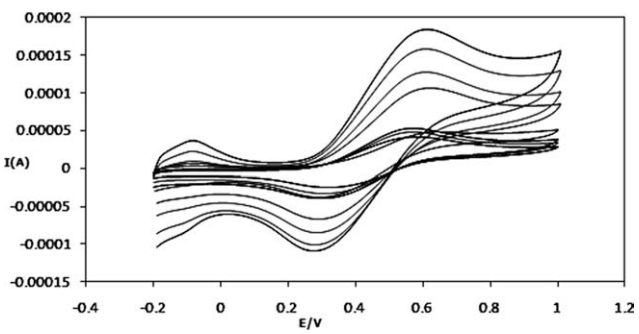

Figure 8 Cyclic voltammetry curves of the HCl-doped solution of poly[aniline-*co*-*N*-(2-hydroxyethyl) aniline]. I: current, E: potential.

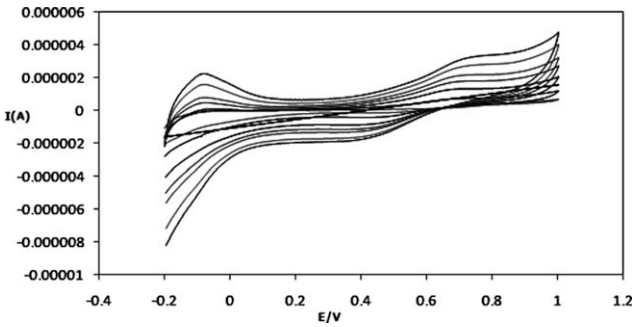

Figure 9 Cyclic voltammetry curves of the HCl-doped solution of the octadecylated copolymer. I: current, E: potential.

HCl. Cyclic voltammetry curves of copolymer samples recorded at different scan rates between −0.2 and 1.0 V versus saturated calomel electrode (SCE) in 1.0M HCl show that they are electroactive polymers. In Figures 8 and 9, the cyclic voltammograms of resultant copolymers exhibit that only one set of redox peaks is observed at (E_{pa}) = 0.63 V for poly[aniline-*co*-*N*-(2-hydroxyethyl) aniline] and E_{pa} = 0.75 for alkylated form (E_{pa} refers to potential of anodic peak). The peaks were ascribed to the oxidation of copolymers. As shown in these figures, *N*-substituted polyaniline exhibited one peak at several scan rates. It could be explained by the decrease in the electroactivity of the obtained polymers after *N*-substitution, which caused the resistance of these polymers to oxidation.[33] Also, in the oxidation step, the alkylated copolymer exhibited a positive shift in the half-potential (E_{pa} = 0.75) compared with poly[aniline-*co*-*N*-(2-hydroxyethyl) aniline] (E_{pa} = 0.63 V). The observation of positive shift in the oxidation might have originated from the steric effect of the side chains. The steric hindrance caused by the side groups could have reduced the Π-conjugation length along the polymer backbone and led to a high oxidation potential.[13]

To increase the electroactivity of the poly[aniline-*co*-*N*-(2-hydroxyethyl) aniline] and octadecylated copolymer films deposited on the electrode, we electropolymerized the aniline on the prepared film. We prepared a 0.1*M* aniline solution with 1*M* HCl and then poured it into the cell. Aniline was electropolymerized in the solution onto the copolymer, which was deposited onto the electrode by the application of a sequential linear potential scan rate between −0.2 and 1.0 V versus SCE; the electrode was then washed with water, and voltammograms were recorded in 1*M* HCl at different scan rates. As shown in Figures 10 and 11, cyclic voltammetry of the unsubstituted copolymer and alkylated copolymer after the electropolymerization of aniline on the related electrode showed two oxidation and reduction peaks, which were due to the addition of aniline in the modified polymer composition. The first and

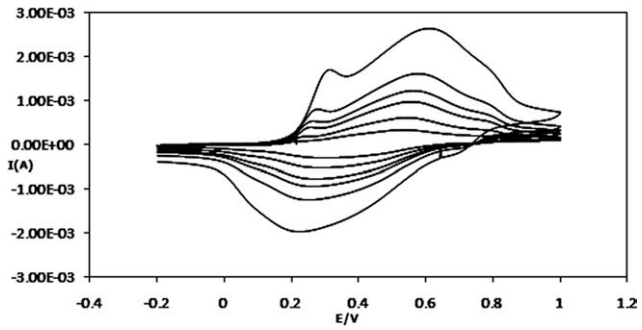

Figure 10 Cyclic voltammetry curves of the HCl-doped film of poly[aniline-*co*-*N*-(2-hydroxyethyl) aniline] after the electropolymerization of aniline. I: current, E: potential.

second oxidation peaks (E_1 and E_2, respectively) of the initial copolymer were characterized at 0.32 and 0.63 V, respectively. $E_1 = 0.37$ V and $E_2 = 0.83$ V were also observed for the alkylated copolymer. The peaks were attributed to polaronic and bipolaronic transitions for the first and second peaks, respectively.[34]

Also, a linear relationship between the anodic and cathodic peak currents versus the scan rate for copolymers before and after the electropolymerization of aniline is shown in Figures 12 and 13. As shown, the slope of the line increased after the electropolymerization of aniline in the copolymers; this confirmed the electroactivity of the modified copolymers. Furthermore, the conductivity of the copolymers was measured by a four-point probe method. The results show that the conductivity of the H_2SO_4-doped poly[aniline-*co*-*N*-(2-hydroxyethyl aniline] was 5×10^{-5} S/cm and that of the octadecyl-substituted copolymer was 5×10^{-7} S/cm. The decrease of the conductivity of the obtained copolymer versus that of than polyaniline was expected to arise from the steric effect of the hydroxyl side groups, which could have provided torsional twists in the polymer backbone and reduced the coplanarity and average electron delocalization length. Such observations were also noted for alkyl-substituted polyaniline.[33]

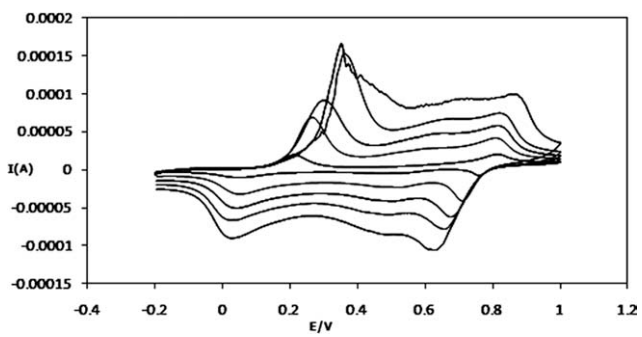

Figure 11 Cyclic voltammetry curves of the HCl-doped film of the octadecylated copolymer after the electropolymerization of aniline. I: current, E: potential.

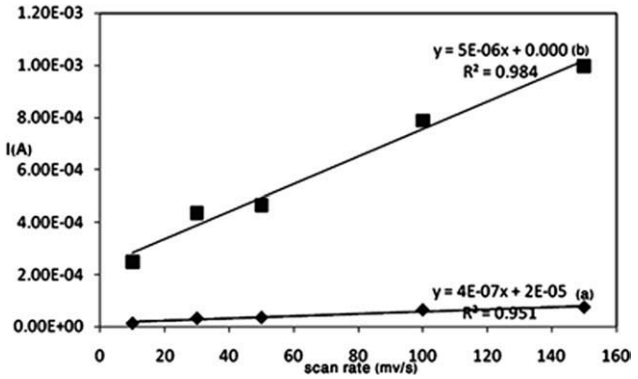

Figure 12 Linear relationship between the current and scan rate of poly[aniline-*co*-*N*-(2-hydroxyethyl) aniline] (a) before and (b) after the electropolymerization of aniline. I: current, E: potential.

CONCLUSIONS

In this article, we have demonstrated that the copolymerization and the incorporation of alkyl substituents may be applied for polyaniline to improve its processability and to modify the physical properties of this conducting polymer. It was shown that it was possible to synthesize poly[aniline-*co*-*N*-(2-hydroxyethyl) aniline] with ammonium persulfate and an octadecylated copolymer by the reaction with octadecyl bromide. FTIR spectroscopy, XRD, and ^{1}H-NMR spectroscopy were helpful in the characterization of the initial copolymer and the alkylated copolymer. The solubility of the initial copolymer was greater than that of polyaniline in organic solvents (NMP and DMF), and also, the solubility was improved remarkably in common organic solvents (chloroform and *n*-hexane) for the octadecylated copolymer. SEM study revealed that there was a significant morphological change in the

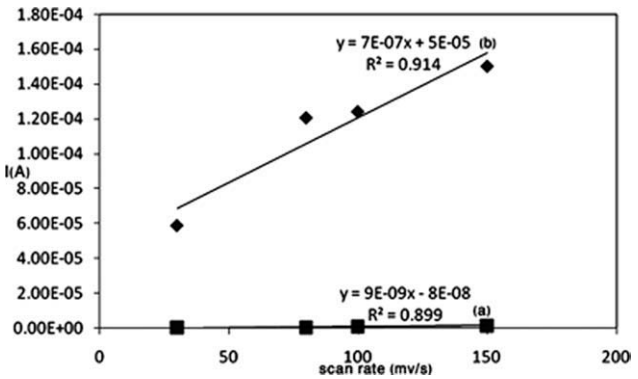

Figure 13 Linear relationship between the current and scan rate of the octadecylated copolymer (a) before and (b) after the electropolymerization of aniline. I: current, E: potential.

unsubstituted copolymer and the alkylated form. The obtained conductivity measured by a four-probe method of H_2SO_4-doped poly[aniline-*co*-*N*-(2-hydroxyethyl) aniline] was 5×10^{-5} S/cm, and that of the octadecyl-substituted copolymer was 5×10^{-7} S/cm. The cyclic voltammetry curves showed that the obtained copolymers were electroactive. The TGA curve of poly[aniline-*co*-*N*-(2-hydroxyethyl) aniline] confirmed the copolymerization of aniline and *N*-(2-hydroxyethyl) aniline, and the performance of alkylated copolymer also was proven. DSC of these copolymers was investigated to determine the copolymerization and alkylation reactions. These results suggest that poly[aniline-*co*-*N*-(2-hydroxyethyl) aniline] could be used as functional copolymer intermediate for the reaction with octadecyl bromide.

References

1. Palaniappan, S.; Amarnath, C. A. React Funct Polym 2006, 66, 1741.
2. Arsata, R.; Yub, X. F.; Li, Y. X.; Wlodarskia, W.; Kalantar-Zadeha, K. Sens Actuators B 2009, 137, 529.
3. Xie, D.; Jiang, Y.; Pan, W.; Li, D.; Wu, Z.; Li, Y. Sens Actuators B 2002, 81, 158.
4. Huang, J.; Virgi, S.; Weiller, B. H.; Kaner, R. Chem A Eur J 2004, 10, 1314.
5. Li, Q.; Wu, J.; Tang, Q.; Lan, Z.; Li, P.; Lin, J.; Fan, L. Electrochem Commun 2008, 10, 1299.
6. Chena, J.; Lia, B.; Zhenga, J.; Zhaoa, J.; Jing, H.; Zhua, Z. Electrochim Acta 2011, 56, 4624.
7. Kim, B. R.; Lee, H. K.; Park, S. H.; Kim, H. K. Thin Solid Films 2011, 519, 3492.
8. Kim, B. R.; Lee, H. K.; Kim, E.; Lee, S. H. Synth Met 2010, 160, 1838.
9. Yoshida, K.; Ning, T.; Masahiro, Y. U.S. Pat. 7,916,455 B2 (2011).
10. Fehse, K.; Schwartz, G.; Walzer, K.; Leo, K. J App Phys 2007, 101, 124509.
11. Jang, J.; Ha, J.; Kim, K. Thin Solid Films 2008, 516, 3152.
12. Cok, R. S.; Boroson, M. L.; O'Toole, R. U.S. Pat. 0190763 A1 (2004).
13. Bajer, I. K.; Zagorska, M.; Niziol, J.; Pron, A.; Luzny, W. Synth Met 2000, 114, 125.
14. Choi, H. J.; Kim, J. W.; Joo, J.; Kim, B. H. Synth Met 2001, 121, 1325.
15. Palaniappan, S.; Nivasu, V. New J Chem 2002, 26, 1490.
16. Xie, H. Q.; Pu, Q. L.; Xie, D. J. J Appl Polym Sci 2004, 93, 2211.
17. Philip, B.; Xie, J.; Abraham, J. K.; Varadan, V. K. Polym Bull 2005, 53, 127.
18. Sudha, J. D.; Sivakala, S.; Prasanth, R.; Reena, V. L.; Radhakrishnan Nair, P. Compos Sci Technol 2009, 69, 358.
19. Martins, C. R.; De Paoli, M. A. Eur Polym J 2005, 41, 2867.
20. Baek, S.; Ree, J. J.; Ree, M. J Polym Sci Part A: Polym Chem 2002, 40, 983.
21. Roy, B. C.; Gupta, M. D.; Bhoumik, L.; Ray, J. K. Synth Met 2002, 130, 27.
22. Lin, D. S.; Yang, S. M. Synth Met 2001, 119, 111.
23. Gok, A.; Sari, B.; Talu, M. Synth Met 2004, 142, 41.
24. Nabid, M. R.; Entezami, A. A. Polym Adv Technol 2005, 16, 305.
25. Mikhael, M. G.; Padias, A. B.; Hall, H. K. J Polym Sci Part A: Polym Chem 1997, 35, 1673.
26. Zheng, W. Y.; Levon, K.; Laakso, J.; Osterholm, J. E. Macromolecules 1994, 27, 7754.
27. Falcoua, A.; Duchenea, A.; Hourquebieb, P.; Marsacq, D.; Balland-Longeau, A. Synth Met 2005, 149, 115.
28. Yanoa, J.; Otab, Y.; Kitani, A. Mater Lett 2004, 58, 1934.
29. Cataldo, F.; Maltese, P. Eur Polym J 2002, 38, 1791.
30. Savitha, P.; Sathyanarayana, D. N. Polym Int 2004, 53, 106.
31. Takayanagi, M.; Katayose, T. J Polym Sci Polym Chem Ed 1981, 19, 133.
32. Hwang, G. W.; Wu, K. Y.; Hua, M. Y.; Lee, H. T.; Chen, S. A. Synth Met 1998, 92, 39.
33. Huang, L. M.; Wen, T. C.; Gopalan, A. Mater Lett 2003, 57, 1765.
34. Gheybi, H.; Bagheri, M.; Alizadeh, Z.; Entezami, A. A. Polym Adv Technol 2008, 19, 967.